Langmuir

Article

pubs.acs.org/Langmuir

Mesophase in a Thiolate-Containing Diacyl Phospholipid Self-Assembled Monolayer

Wangqiang Sun,*[,†,‡,§,#] Sumit Kewalramani,[‖] Karl Hujsak,[‖] Heng Zhang,[†,§] Michael J. Bedzyk,[‖,⊥] Vinayak P. Dravid,[‖] and C. Shad Thaxton*[,†,§]

[†]Department of Urology, Feinberg School of Medicine, Northwestern University, 303 East Chicago Avenue, Chicago, Illinois 60611, United States

[‡]School of Materials Science & Engineering, Hubei University of Technology, Wuhan 430068, China

[§]Simpson Querrey Institute for BioNanotechnology, Northwestern University, 303 East Superior, Chicago, Illinois 60611, United States

[‖]Department of Materials Science and Engineering, Northwestern University, 2220 Campus Drive, Evanston, Illinois 60208, United States

[⊥]Department of Physics and Astronomy, Northwestern University, 2145 Sheridan Road, Evanston, Illinois 60208, United States

[#]Hubei Provincial Key Laboratory of Green Materials for Light Industry, Hubei University of Technology, Wuhan 430068, China

Supporting Information

ABSTRACT: Maintaining the intrinsic features of mesophases is critically important when employing phospholipid self-assemblies to mimic biomembranes. Inorganic solid surfaces provide platforms to support, guide, and analyze organic self-assemblies but impose upon them a tendency to form well-ordered phases not often found in biomembranes. To address this, we measured mesophase formation in a thiolate self-assembled monolayer (SAM) of diacyl phospholipid, 1,2-dipalmitoyl-*sn*-glycero-3-phosphothioethanol (DPPTE) on Au(111), and provide thermodynamic analysis on the mixing behavior of inequivalent DPPTE acyl chains. Our work has uncovered three fundamental issues that enable mesophase formation: (1) Elimination of templating effects of the solid surface, (2) Weakening intermolecular and molecule−substrate interactions in adsorbates, and (3) Equilibrium through entropy-driven self-assembly. Thus, our work provides a more holistic understanding of phase behavior, from liquid phases to mesophases to highly crystalline phases, in organic self-assemblies on solid surfaces, which may extend their applications in nanodevices and to the wider fields of biology and medicine.

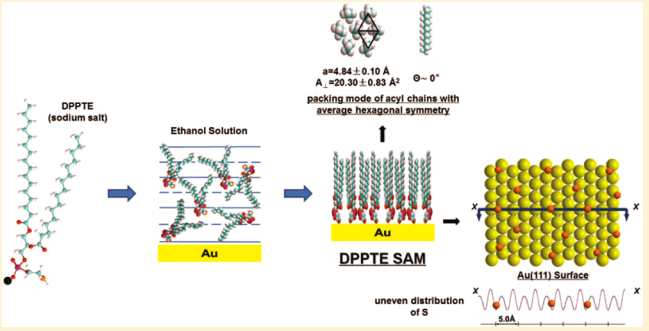

INTRODUCTION

Biomembranes are natural two-dimensional (2D) nanostructures mainly composed of phospholipid bilayers, a common organic self-assembly.[1−3] In condensed matter physics, ordering of anisotropic molecules occurs through the loss of orientational, translational, and rotational freedoms in stepwise fashion in going from liquid phase to mesophases to well-ordered crystalline phases.[4,5] Mesophases of phospholipids are critically important for the activity of biomembranes.[1−3] For example, the lamellar liquid-crystalline phase of phospholipids is found in most membrane regions and domains.[1−3] As another example, the interaction between antimicrobial peptides and bacterial membranes leads to gel-phase domain formation.[6] In short, it is critical to maintain and enable the intrinsic features of mesophases of phospholipids in biomimetic membranes.

Organic molecules are common building blocks for self-assembled structures. However, it is difficult to practically use and analyze freestanding organic self-assemblies. As such, inorganic solid surfaces provide convenient platforms to form and study self-assemblies. In addition to providing support, the surface interacts with the self-assembling molecules.[7−9] Ultimately, stability results from a combination of intermolecular forces and molecule−substrate interactions, whereby typical adsorbates form crystalline phases at well-ordered sites on solid surfaces.[7−9] Highly ordered adsorbates have excellent physical and chemical properties for manufacturing diverse organic nanodevices; however, they are less relevant to biology due to significant restriction of dynamic molecular motion. Recently, loosely packed self-assemblies have been reported that present 2D liquid phases on solid surfaces to avoid these restrictions.[10−12] Notably, many molecules used to form organic assemblies on solid surfaces are anisotropic, like phospholipids. Thus, the mesophase may also be present in these assemblies in terms of the principles of condensed matter

Received: December 12, 2014
Revised: February 12, 2015
Published: February 19, 2015

DOI: 10.1021/la504822q
Langmuir 2015, 31, 3232−3241

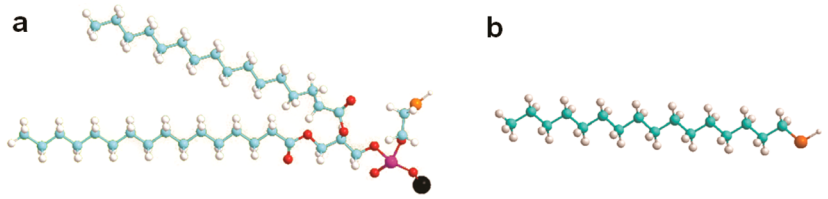

Figure 1. Three-dimensional ball-and-stick models of DPPTE (sodium salt) (a) and 1HT (b). Atomic color codes: red, O; purple, P; orange, S; black, Na; blue-green, C; white, H.

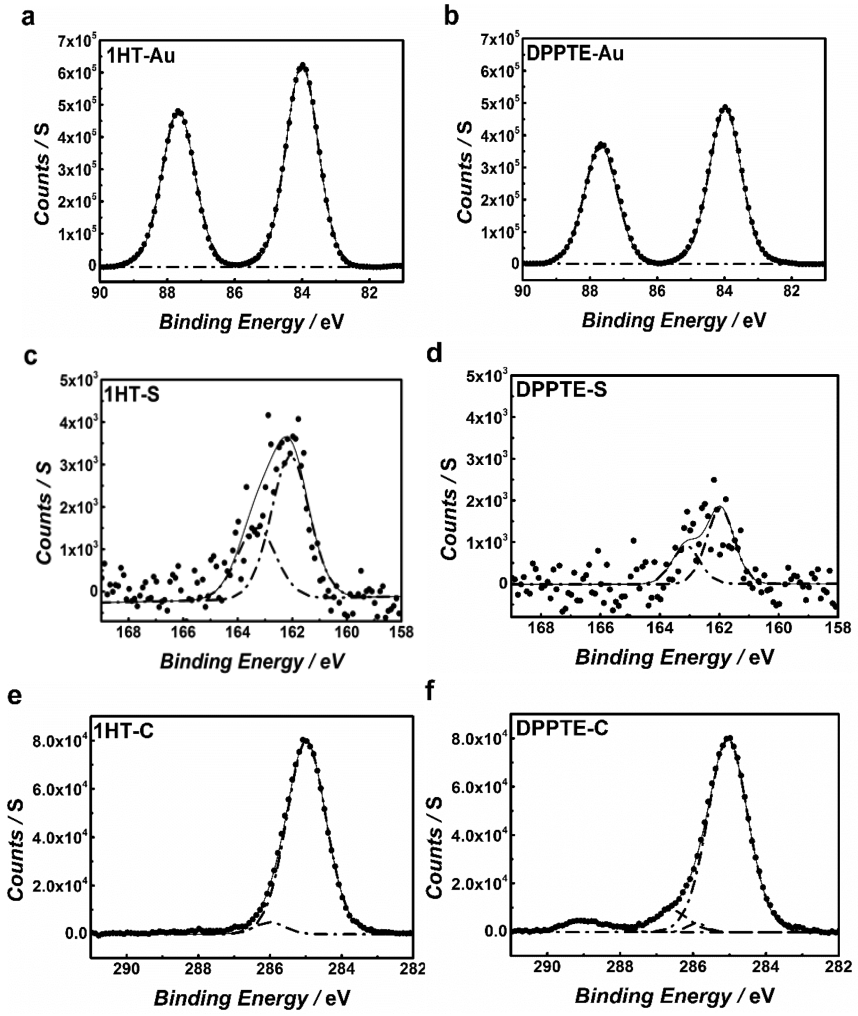

Figure 2. XP spectra for the 1HT SAM and the DPPTE SAM: Au 4f regions of 1HT (a) and DPPTE (b); S 2p regions of 1HT (c) and DPPTE (d); C 1s regions of 1HT (e) and DPPTE (f). In each spectrum, the experimental data (dots) are compared to a simulated spectrum (solid line), which is subdivided into chemically shifted components (dash−dot lines).

physics. Nevertheless, to the best of our knowledge, very few studies have been reported in this area. With a focus on biologically relevant lipids, phospholipids have been shown to directly self-assemble on solid surfaces.[13−20] However, it is still not clear whether or not they form mesophases. Therefore, we were motivated to investigate the structure of a self-assembled phospholipid monolayer on a solid surface and to better understand the general formation mechanism.

As a common substrate used for a number of existing spectroscopies and analytical techniques, gold [especially planar Au(111)] is widely employed for organic self-assemblies. Gold has many additional advantages with regard to the ease with which one can obtain and pattern the substrate, its inert nature, and biocompatibility.[21−25] Due to strong Au−S bonds (~50 kcal/mol), sulfur-containing organic molecules self-assemble on gold to form self-assembled monolayers (SAMs).[21−25] SAMs on Au(111) are among the most commonly investigated organic self-assemblies and provide useful models for studying biological and biochemical processes. In this work, we demonstrate mesophase formation in a SAM composed of a thiolate-containing diacyl phospholipid. Then, thermodynamic analysis reveals that the inequivalent acyl chains of the phospholipid are randomly mixed in the SAM. As a result, we further explore fundamental issues critical to mesophase formation, such as templating effects at the solid surface, interactions in the adsorbate, and the equilibrium mechanism in

DOI: 10.1021/la504822q
Langmuir 2015, 31, 3232−3241

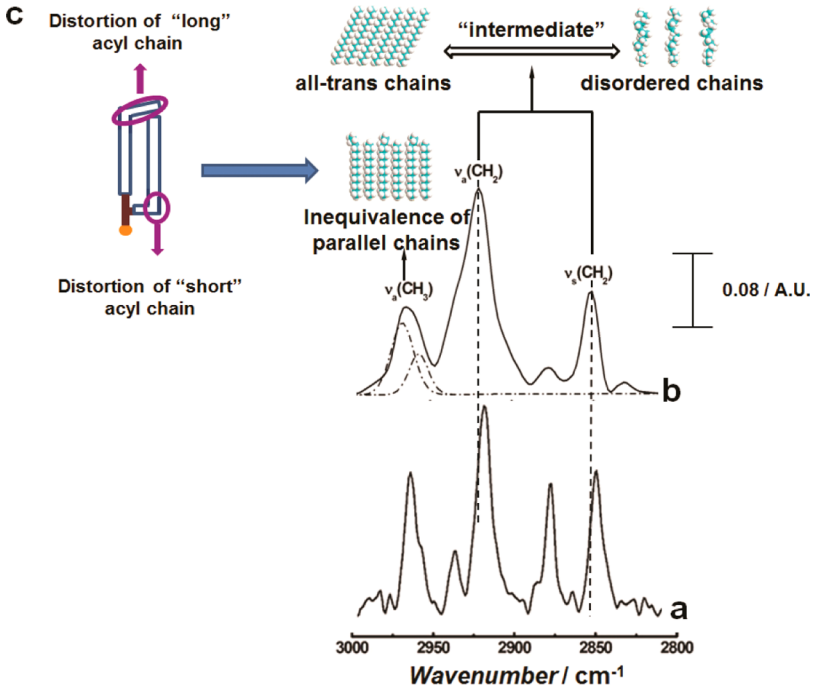

Figure 3. PM-IRRAS of the 1HT SAM (a) and the DPPTE SAM (b) on Au(111) in CH stretching regions. Atomic color codes of space-filling models of *n*-alkyl chains: blue-green, C; white, H. The schematic (c) shows the preferred conformation of diacylglycerol in DPPTE (blank block, acyl chain; brown line, the phospholipid headgroup (including glycerol); orange ball, S atom).

the SAM. As such, this work provides a foundation for forming mesophases in 2D assemblies on solid surfaces and also enhances our understanding of phase behavior of 2D assemblies, from well-ordered crystalline phases to liquid phases.

EXPERIMENTAL SECTION

Materials and Methods. 1,2-Dipalmitoyl-*sn*-glycero-3-phosphothioethanol [DPPTE, sodium salt, as lyophilized powder (>99%)] and 1-hexadecanethiol (1HT, ≥95.0%) were purchased from Avanti Polar Lipids and Sigma-Aldrich, respectively. The Au(111) substrates with a thickness of 1000 Å over a titanium adhesion layer on silicon wafers were purchased from Platypus Technologies. The predominantly presented Au(111) face was confirmed by XRD. To form the DPPTE SAM and the 1HT SAM, the Au(111) substrates, which were cut into different sized pieces and rinsed with pure ethanol by sonication, were immersed into a freshly prepared 1 mM solution of DPPTE or 1HT in ethanol for a prolonged time of 72 h at 298 K. Next, the samples were removed from the solution, rinsed thoroughly with pure ethanol, and then dried under a flow of nitrogen. Finally, all samples were stored under vacuum. The samples were further characterized by polarization modulation infrared reflection absorption spectroscopy (PM-IRRAS), contact angle, X-ray photoelectron spectroscopy (XPS), tapping mode atomic force microscopy (TM-AFM), and grazing incidence X-ray diffraction (GIXRD) (Supporting Information).

RESULTS AND DISCUSSION

Formation and Structure of the DPPTE SAM on Au(111). Diacyl phospholipids are important amphiphilic lipids that make up biomembranes and are essential for life.[1−3] It has been reported that some ordinary phospholipids easily present in the mesophase in monolayers formed at water−air interfaces, where their headgroups tend to misalign and do not coincide with the ordering of the acyl chains.[26] In the context of SAMs, sulfur-containing diacyl phospholipids have been used to functionalize gold surfaces.[13−20] Since sulfur-containing diacyl phospholipids are molecularly similar to ordinary phospholipids, it is assumed that they form SAMs on gold with mesophases that are similar to those found in lamellar self-assemblies of phospholipids. However, to date, there are very few reports analyzing the structure of SAMs formed using a sulfur-containing diacyl phospholipid.[27] DPPTE is a simple, commercially available, thiol-containing diacyl phospholipid (Figure 1a), which readily forms a SAM on gold. Thus, we employed DPPTE to investigate mesophase formation.

SAMs of *n*-alkyl thiolates on Au(111) are critically important archetypes in the field of SAMs. They present crystalline-like domains of dense and stable hexagonal $(\sqrt{3} \times \sqrt{3})R30°$ lattices relative to the (1 × 1) unit cell of the gold and its c(4 × 2) superlattice, which provides a foundation to understand SAMs on Au(111).[21−25] 1HT is a typical *n*-alkyl thiol with the same length hydrocarbon chain as in the DPPTE molecule (Figure 1b). This molecule was used to form an *n*-alkyl thiolate SAM for comparison to the SAM formed from DPPTE.[1,2]

The formation of the 1HT and DPPTE SAMs on Au(111), essentially free of water or ethanol, was demonstrated by PM-IRRAS (Supporting Information, Figure S1), contact angle $\theta_a(H_2O)$ [advancing contact angle for water under air] (Supporting Information), and XPS (Figure 2, Supporting Information, Figure S2). From Figure 2a and 2b, XPS data demonstrate both the 1HT and the DPPTE SAMs have an Au $4f_{7/2}$ peak at 83.98 eV that can be assigned to the "bulk" Au component.[28,29] The S 2p spectra of either the 1HT SAM (Figure 2c) or the DPPTE SAM (Figure 2d) can be fitted with two spin−orbit coupled components (each with area ratios of 2:1 and splittings of 1.2 eV) located at ∼162.0 or 163.2 eV corresponding to the thiolate group, respectively.[28,29] Figure 2e indicates that the C 1s spectrum of the 1HT SAM can be separated into two peaks located at 284.99 and 286.01 eV, corresponding to the C−H and C−S bonds[28,29] in the 1HT molecule (Figure 1b). Figure 2f illustrates that the C 1s spectrum of the DPPTE SAM can be separated into four peaks

DOI: 10.1021/la504822q
Langmuir 2015, 31, 3232−3241

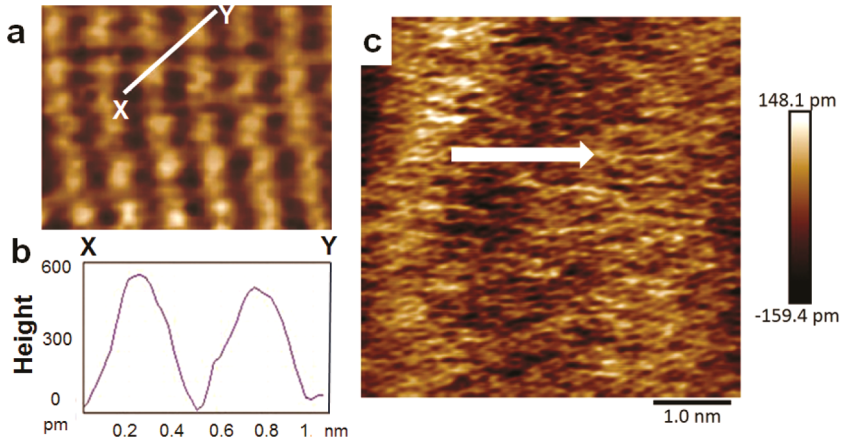

Figure 4. Color TM-AFM images of SAMs on the Au(111) surface obtained in air. (a) 1HT SAM, 3 nm × 2 nm, Δf = 1326 Hz, v_{tip} =12 nm/s. (b) Cross-sectional plot measured along a black line $X-Y$ in (a). (c) DPPTE SAM, 4.5 nm × 4.5 nm, Δf = 1326 Hz, v_{tip} = 22 nm/s.

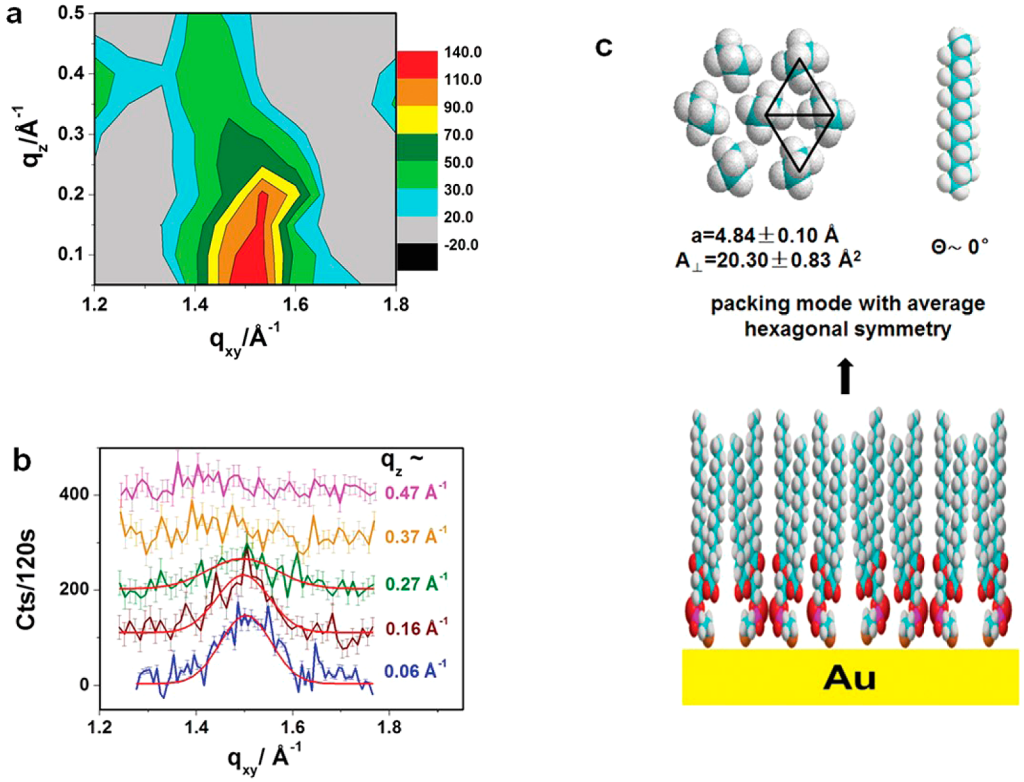

Figure 5. Packing mode of the backbone of acyl chains in the DPPTE SAM. (a) 2D Contour plots of GIXRD intensity as a function of the surface-parallel (q_{xy}) and surface-normal (q_z) components of the scattering vector for the DPPTE SAM on Au. (b) Grazing incidence X-ray scattering for DPPTE SAM on Au(111) as a function of q_{xy} at different q_z. (c) Schematic illustration of disordered R_{II} packing mode in the DPPTE SAM. Here, a is the lattice constant and $A_\perp$ the cross sectional area per chain perpendicular to the long axes; Θ is the tilt angle of the DPPTE chains with respect to substrate normal (top, right). Atomic color codes of the space-filling model and three-dimensional ball-and-stick model of DPPTE molecule: red, O; purple, P; orange, S; black, Na; blue-green, C; white, H.

located at 285.04, 285.91, 286.59, and 288.91 eV corresponding to C−H, C−S, C−O, and O−C═O bonds[30,31] in DPPTE molecule (Figure 1a), respectively.

Next, we further compared the structures of SAMs formed from 1HT and DPPTE. Our results reveal that, as a typical *n*-alkyl thiolate SAM, the 1HT SAM displays features corresponding to crystalline domains of dense and stable hexagonal ($\sqrt{3} \times \sqrt{3}$)R30° lattices:[21−25] (1) Sharp symmetric $\nu_s(CH_2)$ and asymmetric $\nu_a(CH_2)$ stretches located at 2849 and 2918 cm^{-1} (Figure 3a), respectively;[32−34] (2) A primary sharp peak of the asymmetric $\nu_a(CH_3)$ stretch located at 2964 cm^{-1} [in-plane component, $\nu_a(CH_3$, ip)] with a small shoulder at 2958 cm^{-1} [out-of-plane component, $\nu_a(CH_3$, op)] (Figure 3a);[35,36] (3) Contact angle θ_a(HD) [advancing contact angle for HD (hexadecane) under air] = 45.94 ± 0.08° revealing an oleophobic surface due to the densely packed CH_3 groups at the outer surface;[37,38] (4) Molecular stripes with an average spacing of ∼0.50 nm presented at the outer surface [color TM-AFM images (Figure 4a and 4b)].[39,40] However, the DPPTE SAM does not show such features and illustrates some intermediate features: (1) Broad $\nu_s(CH_2)$ and $\nu_a(CH_2)$ bands located at 2851 and 2920 cm^{-1} (Figure 3b) between those of

DOI: 10.1021/la504822q
Langmuir 2015, 31, 3232−3241

Table 1. Comparison of Structure Parameters of SAMs[a]

SAMs	a (Å)	S_C (Å^2)[b]	R_C	S_M (Å^2)[b]	R_s	$A_\perp$ (Å^2)
n-alkyl thiol	5.0[c]	21.6	1	21.6	1	18.4[c]
DPPTE	4.84 ± 0.10	20.30 ± 0.83	~1.064	40.60 ± 0.83	~0.532	20.3 ± 0.83

[a] a, lattice constant; S_C, the area of a chain at the layer surface; R_C, ratio of the coverage of chains; S_M, the area of a molecule at the layer surface; R_s, ratio of the coverage of thiolates; $A_\perp$, cross-sectional area per chain perpendicular to the long axes. [b] Calculated from a. [c] Quoted from reference 22.

the well-ordered crystalline and isotropic liquid states, respectively;[32−34] (2) A broad peak of the $\nu_a(CH_3)$ stretch that can be deconvoluted into two overlapping bands with maxima at 2958 and 2967 cm^{-1}, interpreted as $\nu_a(CH_3$, op) and $\nu_a(CH_3$, ip) components, respectively (Figure 3b);[35,36] (3) $\theta_a(HD) = 34.85 \pm 0.30°$ between the contact angles measured for well-ordered and disordered mixed *n*-alkyl thiolate SAMs;[37,38] (4) Only the terminals of hydrocarbon chains lying down along the white arrow in color TM-AFM image in Figure 4c observed at the outer surface of the DPPTE SAM.

The measured differences between the DPPTE and the 1HT SAMs prompted us to acquire packing parameters for the DPPTE SAM by GIXRD.[41,42] Shown in Figure 5a and 5b, there is one first-order peak for the DPPTE SAM, which decays with increasing q_z. The appearance of a single first-order diffraction peak corresponds to a hexagonal lattice. The peak maximum intensity is projected to be at $q_z \approx 0$ Å^{-1}, which implies the tilt angle of the hydrocarbon chains $\Theta \approx 0°$(Figure 5c).[41−43] From the in-plane position, $q_{xy} = 1.50 \pm 0.03$ Å^{-1}, the lattice constant (a) and the cross-sectional area per chain perpendicular to the long axes ($A_\perp$) can be determined as 4.84 ± 0.10 Å and 20.30 ± 0.83 Å^2 (Figure 5c, Table 1), respectively. These data show that the acyl chains in the DPPTE SAM are less densely packed than previously reported[27] and may be packed in a hexagonal rotator phase (R_{II}, the free rotator phase with the highest symmetry) because $A_\perp$ is close to 19.8 Å^2, the value for regular R_{II} of pure *n*-alkanes.[26,44,45] It should be noted that in phospholipids, acyl chains cannot freely rotate about their long axes.[26] Meanwhile, the peaks are broader than the resolution (Figure 5b). Therefore, our data suggest that in DPPTE monolayers there is sufficient static disorder in the molecular orientation, such that on average acyl chains can be approximated as cylindrically symmetric, similar to that of ordinary phospholipid monolayers with small headgroups in the gel phase.[6,26,41] Second, unlike *n*-alkyl SAMs[21−25] (Table 1), a $(\sqrt{3} \times \sqrt{3})$R30° epitaxial relationship between 2D lattices of hydrocarbon chains and the Au(111) unit cell does not exist. For a $(\sqrt{3} \times \sqrt{3})$R30° lattice the diffraction peaks are expected at $q_{xy} = 1.45$ Å^{-1}.

In ordinary *n*-alkyl thiolate SAMs, outer surfaces are mainly composed of densely packed CH_3 groups.[21−25] However, it has been reported that double acyl chains in phospholipids have a tendency to orient parallel to each other regardless of whether they are assembled in crystalline or mesophase states (Figure 3c).[46−48] In this preferred conformation of diacylglycerol, one acyl chain has to bend, which results in it being "shorter" than the other extended chain along the molecular axis.[46−48] Overall, the straight "long" acyl chain becomes distorted near its terminal CH_3 group due to the absence of lateral interaction, while the bent "short" chain is more ordered at its end through contact with "long" chains.[46−48] Generally, $\nu_a(CH_3$, op), which occurs prominently in the polycrystalline bulk phase spectra, is very weak in the monolayer spectra at room temperature.[35,36] The more obvious occurrence of $\nu_a(CH_3$, op) in the DPPTE SAM may be unique to bent "short" chains (Figure 3b). Ultimately, the inequivalence of double acyl chains in DPPTE suggests the outer surface of the DPPTE SAM is mainly composed of the protruded terminal of the "long" chain. This feature corresponds well to the TM-AFM image depicted in Figure 4c.

Mixing Behavior of Acyl Chains of the DPPTE SAM. It is notable that *n*-alkyl thiols with enough difference in chain lengths are immiscible in mixed SAMs.[49,50] As discussed, the preferred conformation of diacylglycerol leads to diacyl chains having inequivalent lengths in the DPPTE SAM. This prompted us to compare the DPPTE SAM with SAMs formed from two-component mixtures of *n*-alkyl thiols that have different chain lengths to understand their mixing behavior. There are two types of equilibria that need to be considered during the formation of a SAM of mixed *n*-alkyl thiols:[51] (1) The equilibrium between the SAM and the solution containing free thiol(s) during SAM assembly and (2) the equilibrium within the SAM that contains the two components at fixed composition after leaving solution. In both cases, the pairing constraint imparted by the phospholipid headgroup leads to energetic penalties in the DPPTE SAM as compared to the case of SAMs formed from mixtures of *n*-alkyl thiols, as follows (Figure 6).

Equilibrium 1 can be described by the model proposed by Folkers et al.[51,52] by employing an equivalent system of a mixed *n*-alkyl thiolate SAM (Figure 6a, Supporting Information). Accordingly, in that mixed system, the ratio between the "long" and the "short" chains in the resulting SAM should not be 1:1 at theoretical equilibrium. However, because of the pairing constraint, the ratio of the acyl chains in the DPPTE SAM has to be 1:1. Therefore, the "theoretical equilibrium" between the DPPTE SAM and the molecules in solution cannot be reached. As a result and according to the commonly assumed surface-collision-controlled (kinetic) limit,[53] the two inequivalent acyl chains are expected to have a random statistical distribution in the DPPTE SAM (i.e., well mixed).

For equilibrium 2, after leaving solution and in the dry state, the DPPTE SAM has a much larger exposed surface area at the outer surface due to the inequivalent acyl chains. The resulting high surface energy cannot be offset by the mixing entropy of the two inequivalent acyl chains in the DPPTE SAM (Supporting Information, Figure S3). Normally, demixing of lipid monolayers serves to reduce the surface energy (Figure 6b). For example, in Langmuir monolayers composed of two immiscible components with single alkyl chains, macroscopic phase separation is observed at equilibrium due to the lateral diffusion of alkyl chains.[51,53] However, in conventional mixed SAMs, the lateral diffusion of alkyl chains is confined by Au−S interactions. The tendency toward microscopic phase separation has been predicted theoretically and observed for mixed SAMs formed from *n*-alkyl thiols.[53] In the DPPTE SAM, the acyl chains are confined both by being bound to their common headgroup and by Au−S interactions. As such, it is difficult for the inequivalent acyl chains within the DPPTE SAM to achieve equilibrium through phase separation.

DOI: 10.1021/la504822q
Langmuir 2015, 31, 3232−3241

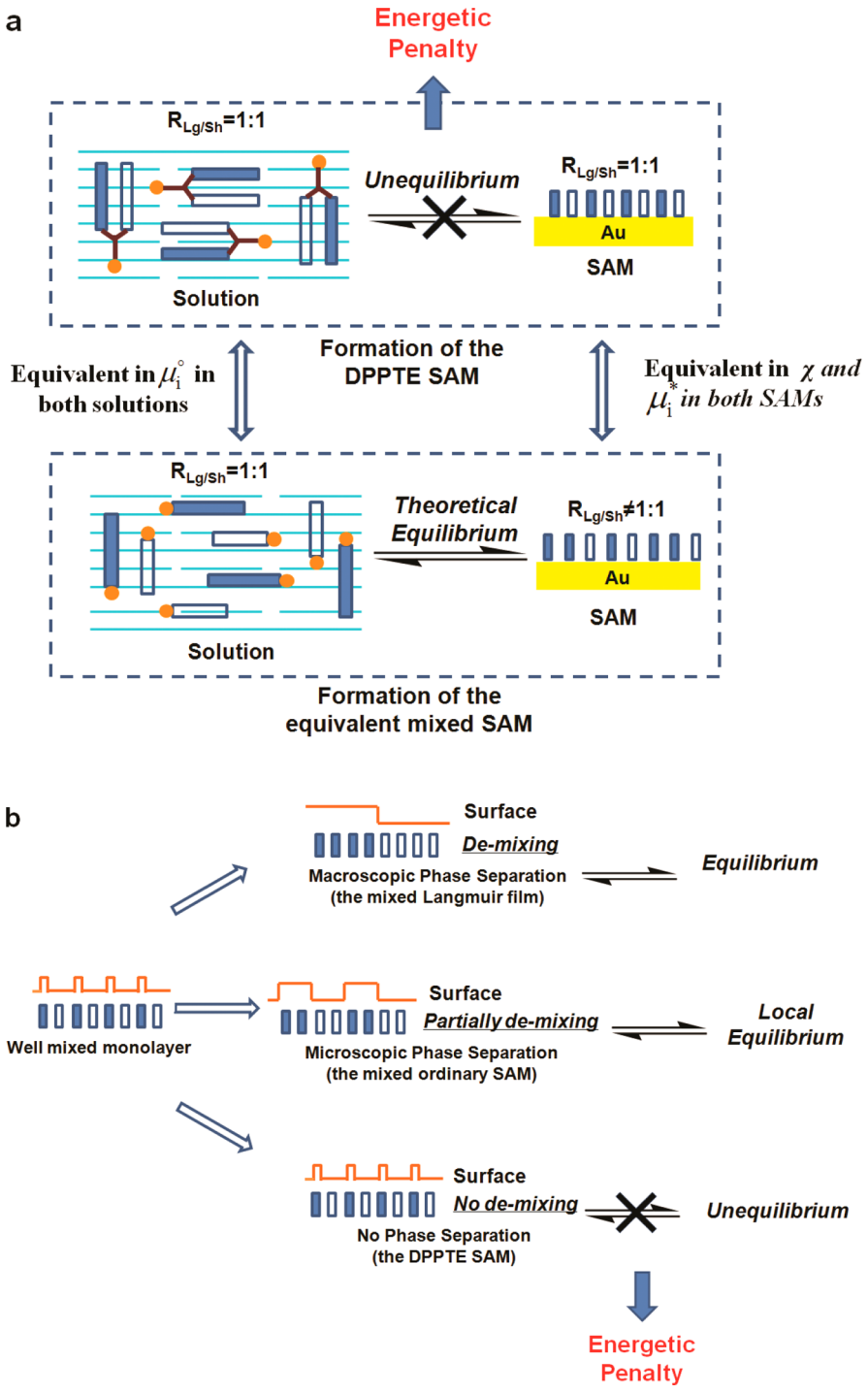

Figure 6. Schematic illustrations of the mixing behavior of acyl chains in the DPPTE SAM on Au(111). (a) Energetic penalty that results during SAM assembly. For DPPTE, the two acyl chains are equivalent in solution but inequivalent in the SAM. An equivalent system consisting of mixed binary−component alkyl thiols is shown to reflect the theoretical equilibrium of the DPPTE SAM. In the latter system, $R_{Lg/Sh}$ [the ratio between the "long" (Lg) and "short" (Sh) chains] in solution and μ_i° (the reference chemical potential at infinite dilution of the "long" or "short" chains are equal) are the same as those for DPPTE corresponding to the equivalence of the two acyl chains of DPPTE while in solution. Meanwhile, the mixed SAM has the same χ (interchange energy parameter) as that of the DPPTE SAM, and μ_i^* (the reference chemical potential in the monolayer for the "long" and "short" chain, which are not equal) for each single chain is equal to that of the DPPTE SAM corresponding to the inequivalent acyl chains in the DPPTE SAM. (b) Energetic penalty introduced after leaving solution. Solid block: the "long" chain (Lg); blank block: the "short" chain (Sh); brown line: phospholipid headgroup (including glycerol); orange ball: S atom.

Breaking the Template Effect on the Au(111) Surface: Disorder of Headgroups in the DPPTE SAM. Lamellar self-assemblies of hydrated phospholipids are formed on the surface of water, which provides an ideally planar (uncorrugated) substrate with weak hydrogen-bond interactions (Figure 7a).[3] However, even atomically flat Au(111) is energetically heterogeneous with an energetic difference (ΔE) of ~6.0 kcal/mol from the peaks to valleys on the surface (Figure 7b).[21]

DOI: 10.1021/la504822q
Langmuir 2015, 31, 3232−3241

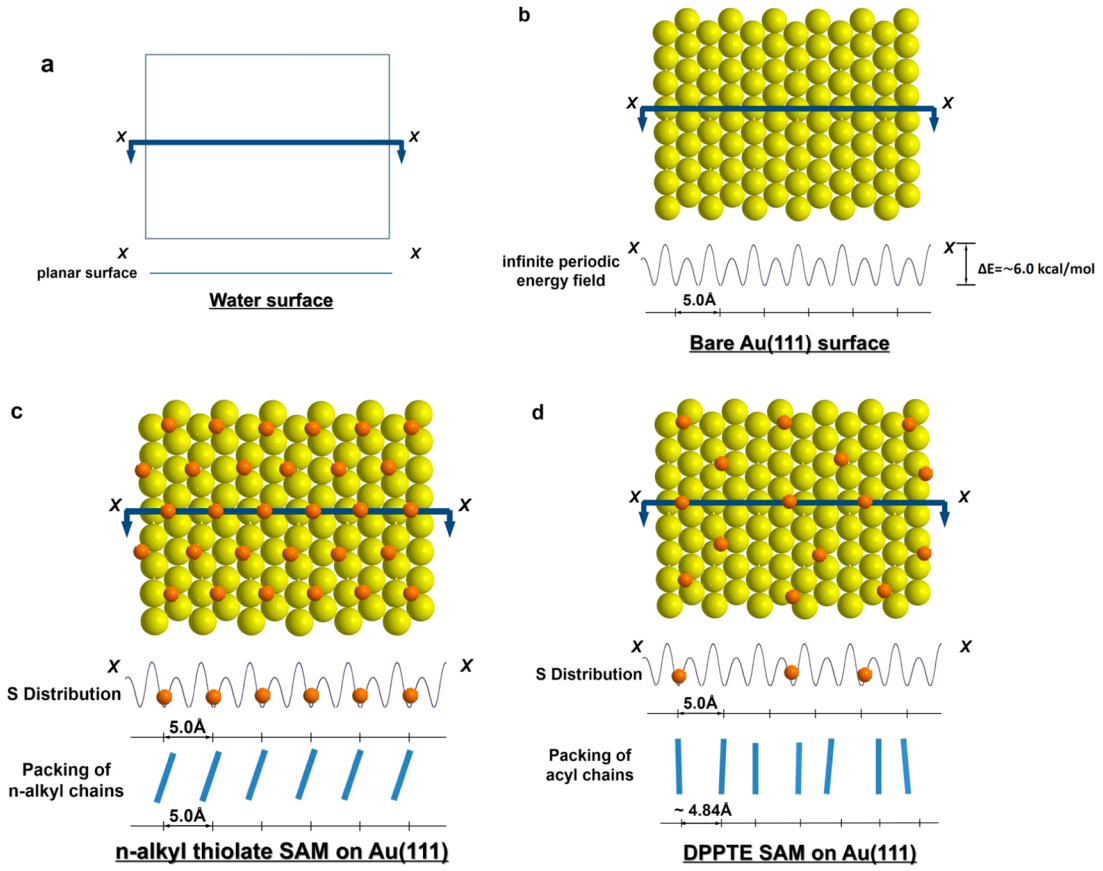

Figure 7. Schematic illustrations of the influence of the template effect at the Au(111) surface. (a) Water surface. (b) Bare Au(111) surface. (c) *n*-Alkyl thiolate SAM on Au(111). (d) DPPTE SAM. Blue line, surface; small orange ball, S atom; big yellow ball, Au atom; blue solid block, *n*-alkyl or acyl chain.

As such, a template effect occurs on the Au(111) surface with an infinite periodic field. For instance, in ordinary *n*-alkyl thiolate SAMs, S evenly distributes with a strict S-to-Au ratio of 1:3 on Au(111) in a $(\sqrt{3} \times \sqrt{3})R30°$ lattice, which is the same as that of the *n*-alkyl chains (Figure 7c).[21−25] This eliminates the influence of energetic heterogeneity and minimizes energy at the Au(111) surface. Therefore, it is necessary to tailor the template effect when forming phospholipid monolayers with mesophases on Au(111).

From Table 1, the ratio of the coverage of thiolates (R_s) between the DPPTE SAM and the *n*-alkyl SAM is ~0.532:1, which means there is a reduction in the density of S in the DPPTE SAM by about one-half when compared with the *n*-alkyl thiolate SAM. This inference is also supported by XPS data (Figure 2e and 2f, Supporting Information), where the ratio of the intensities of the detected S photoelectrons for the DPPTE SAM and the 1HT SAM, $S(2p)_{DPPTE}/S(2p)_{1HT}$, is 0.464. The slight difference (from 0.532 to 0.464) between the GIXRD and the XPS-derived relative S coverage arises because in XPS the S photoelectrons are more easily attenuated in the DPPTE SAM than in the 1HT SAM due to the increased thickness of the DPPTE SAM (Supporting Information). In addition to the reduced density of S in DPPTE SAM, the acyl chains in the DPPTE SAM are actually presented in a disordered R_{II}, where they may locally pack in a distorted structure and not regularly orient normal to the surface. The lattice parameter of the DPPTE SAM, $a = 4.84 \pm 0.10$ Å, is smaller than that of the *n*-alkyl thiolate SAM, $a = 5.0$ Å (Figure 5c, Table 1). These findings suggest that the S arrangement in the DPPTE SAM is likely not commensurate with the Au(111) substrate in the DPPTE SAM. Therefore, DPPTE molecules likely arrange on Au(111) to optimize changes in corrugation energy and may not evenly distribute on Au(111) as is the case in *n*-alkyl thiolate SAMs. Ultimately, the best way for the S in DPPTE to bind to Au(111) is by neglecting positional order to overcome energy barriers that result from surface corrugation (Figure 7d).

Of note, DPPTE has a special molecular structure where there are two acyl chains attached to a single headgroup through the glycerol linker. Certainly, the diacyl chains may lead to increased steric hindrance (Figure 1a). The results correspond well with the special molecular structure of DPPTE. Therefore, the template effect on the Au(111) is broken due to the steric restriction of diacyl chains. Finally, disorder of the DPPTE headgroups would undoubtedly increase the system energy when compared with crystalline-like *n*-alkyl thiolate SAMs. Thus, this arrangement leads to another energetic penalty to stable DPPTE SAM formation.

Interactions in the DPPTE SAM. Generally, the 2D arrangement of organic molecules on solid surfaces is the result of a combination of intermolecular forces and molecule−substrate interactions.[7] In *n*-alkyl thiolate SAMs, both of these interactions are very strong.[21−25] Au−S bonds direct the *n*-alkyl chains to be arranged in a hexagonal $(\sqrt{3} \times \sqrt{3})R30°$ lattice. Consequently, van der Waals forces between *n*-alkyl chains are maximized such that *n*-alkyl chains obtain rotational and orientational orders.[21−25] In loosely packed SAMs, the reduced density of alkyl chains results in a reduction of van der Waals

DOI: 10.1021/la504822q
Langmuir 2015, 31, 3232−3241

forces and leads to a 2D liquid state.[10] Further, *n*-alkyl chains in SAMs of dialkylsulfides are densely packed in a stable hexagonal lattice with a lattice parameter of ~4.5 Å, which is nearly equal to the close-packed structure of alkyl chains and even smaller than that observed for common *n*-alkyl thiolate SAMs.[54] Here, van der Waals forces between *n*-alkyl chains are maximized to maintain equilibrium despite reduced molecule−substrate interactions imparted by physisorption rather than chemisorption.

In the DPPTE SAM, the interplay between intermolecular forces and molecule−substrate interactions is different and both interactions are weakened. First, the density of Au−S bonds on the Au(111) surface has been reduced to about one-half, which proportionately reduces the total molecule−substrate interactions. Next, thermodynamic analysis above illustrates that inequivalent acyl chains of DPPTE are immiscible. Due to restriction of the preferred conformation by diacylglycerol and the immobilization due to Au−S bonds, immiscible acyl chains cannot be separated and have to be well mixed. Thus, the intermolecular van der Waals interactions cannot be maximized, even though the density of acyl chains is higher than that of *n*-alkyl chains in common *n*-alkyl thiolate SAMs (ratio of the coverage of hydrocarbon chains between the DPPTE SAM and the *n*-alkyl thiolate SAM, $R_C = 1.064 > 1$, Table 1). As a result, the intermolecular interactions have to be weakened, too.

In addition, DPPTE has a negative phosphate group. XPS data suggest that the Coulomb interactions from phosphates in the DPPTE SAM are not completely screened by the Na^+ counterion and may inhibit neighboring molecules from approaching each other[46] (Supporting Information, Figure S2b and S2c). On the other hand, it is widely known that the phosphate group easily combines small polar molecules through the hydrogen bond.[46] However, XPS spectrum does not reveal signal from hydroxyl groups (Supporting Information, Figure S2a), which implies that there is no water or ethanol, the solvent used for DPPTE SAM formation.

Equilibrium Mechanism in the DPPTE SAM. Self-assembly is an automatic ordering process under equilibrium conditions. According to the second law of thermodynamics there are two ways to decrease the free energy in a system:[55] (1) Through energetically favorable attractive interactions, which are sensitive to temperature-driven phase transitions, and (2) through entropy-related volume interactions driven by density instead of temperature. Correspondingly, both modes occur in thiolate SAMs on gold. The first appears in common *n*-alkyl thiolate SAMs on Au(111), while the second presents in striped mixed SAMs on curved surfaces of nanostructures.[49,50] Altogether, there are two energetic penalties in the DPPTE SAM, one originating from the mixing behavior of acyl chains and the other from the disorder of the headgroup at the Au(111) interface. In order for the DPPTE SAM to be stable at room temperature, the energetic penalties must be offset to decrease the free energy in the DPPTE SAM. However, both free rotation of the chains about their long molecular axes and the lateral motion of double chains are hindered due to the pairing of the double acyl chains to their common headgroup. Ultimately, optimization of attractive interactions is difficult in the DPPTE SAM and entropic effects become uniquely capable of decreasing the free energy.

Notably, acyl chains in the DPPTE SAM present in a special disordered R_{II}, where positional, rotational, and orientational freedoms are partially maintained. Forming a disordered R_{II} becomes one efficient way for acyl chains to offset energetic penalties in the DPPTE SAM. Next, data show that the cross section for each terminal of the "long" chain at the outer surface of the DPPTE SAM doubles that of a single chain to ~40.6 $Å^2$ (Table 1), which provides enough space for the "long" chain to bend over a neighboring "short" one. Similar to striped mixed SAMs on curved surface of nanostructures,[49,50] the conformational entropy gain in the terminal of the "long" chain may further offset energetic penalties in the DPPTE SAM.

SUMMARY

Ultimately, our data show that the SAM formed by DPPTE is the result of the intrinsic mixing of individual, nonequivalent acyl chains, which leads to the formation of a novel mesophase, disordered R_{II}. In the DPPTE SAM, the nonequivalent acyl chains cannot phase separate nor can there be deviation from a strict 1:1 ratio of "long" to "short" chains due to their coupling to a common molecular headgroup. For DPPTE SAM formation, like *n*-alkylthiolate SAMs, stability results from an interplay between intermolecular and headgroup−substrate interactions. However, unlike for common *n*-alkylthiolate SAMs where these interactions are maximized, our data and analysis support an assembly mechanism and subsequent stability in the DPPTE SAM that results from an energetic minimum found by optimizing and balancing these interactions. As a result, the behavior of the DPPTE SAM is different from that of common *n*-alkylthiolate SAMs.

More broadly, biomembranes have been a topic of considerable interdisciplinary research and debate for decades. In order to increase our understanding of biomembranes, it is necessary to set up close connections with physical and chemical model systems. This work shows that the SAM of a thiolate-containing diacyl phospholipid may provide a platform to understand the thermodynamics of the mixing behavior of inequivalent acyl chains of phospholipids, the key building blocks of biomembranes. Both the DPPTE SAM and the gel-phase monolayers of ordinary phospholipids with small headgroups have a similar disordered R_{II} packing mode of the chain backbones resulting from headgroup disorder. The close similarity between them may encourage further exploration of thiolate-containing phospholipid SAMs with mesophases to more accurately mimic biomembranes.

Finally, self-assembly is an autonomous process whereby disordered systems become ordered under equilibrium conditions through noncovalent interactions. For a molecule with an anisotropic shape, ordering occurs stepwise. Correspondingly, self-assemblies of anisotropic molecules may exhibit features of hierarchical ordering. In general, organic self-assemblies have a tendency to form well-ordered phases on inorganic solid surfaces. Meanwhile, 2D liquid phases have been reported in loosely packed self-assemblies on solid surfaces by decreasing the density of adsorbates. In short, our work has uncovered three fundamental issues that enable mesophase formation: (1) Elimination of templating effects at the solid surface, (2) weakening intermolecular and molecule−substrate interactions in adsorbates, and (3) equilibrium through entropy-driven self-assembly. As such, this work may provide a bridge to understanding the connections between well-ordered crystalline phases and liquid phases in 2D assemblies on solid surfaces. Thus, this work not only provides evidence of previously unmeasured new phases in thiolate SAMs but also enhances our understanding of phase behavior of 2D assemblies as a whole.

DOI: 10.1021/la504822q
Langmuir 2015, 31, 3232−3241

■ ASSOCIATED CONTENT

Supporting Information

Methods of PM-IRRAS, contact angle, XPS, TM-AFM, and GIXRD; transmission FTIR spectra of DPPTE powder and 1HT in carbon tetrachloride solution; XP spectra for the DPPTE SAM; schematic illustration of the free energy of DPPTE in the SAM, neglecting the confinements from the Au−S interaction and pairing constraint of phospholipid headgroup; more details of the formation of SAMs and the thermodynamic analysis. This material is available free of charge via the Internet at http://pubs.acs.org.

■ AUTHOR INFORMATION

Corresponding Authors

*E-mail: cthaxton003@md.northwestern.edu.
*E-mail: swqpeter@163.com.

Author Contributions

W.S., H.Z., and C.S.T. conceived the research and designed the experiments. W.S., S.K., and K.H. conducted the experiments and analyzed the data. W.S., S.K., K.H., M.J.B., V.D., and C.S.T. interpreted the data. W.S. and C.S.T. wrote the manuscript. All authors read and provided input to the final manuscript.

Notes

The authors declare no competing financial interest.

■ ACKNOWLEDGMENTS

We thank Dr. Xinqi Chen at the Keck Interdisciplinary Surface Science Center, Northwestern University, and Professor Franz Geiger and Ms. Mary Alice Upshur, Department of Chemistry, Northwestern University, for technical assistance. Also, we acknowledge Professors George Schatz and Khalid Salaita and Dr. Cheng-Tsung Lai for their review of the manuscript and helpful discussions. For financial support we thank the Howard Hughes Medical Institute (HHMI) for a Physician Scientist Early Career Award, the Department of Defense/Air Force Office of Scientific Research (FA95501310192 and FA9550-11-1-0275), the National Institutes of Health/National Cancer Institute (U54CA151880 and R01CA167041), the State Scholar Fund of China Scholarship Council (Grant No. z2009842363), and the Science and Technology Project (Major Program) of Hubei Provincial Education Department, China (Grant No. z20081401). Finally, the NSF-MRSEC program through the Northwestern Materials Research Center (DMR-1121262) supported use of the J. B. Cohen X-ray Diffraction Facility.

■ REFERENCES

(1) Edidin, M. Lipids on the Frontier: A Century of Cell-Membrane Bilayers. *Nat. Rev. Mol. Cell Biol.* **2003**, *4*, 414−418.
(2) Simons, K.; Vaz, W. L. C. Model Systems, Lipid Rafts, and Cell Membranes. *Annu. Rev. Biophys. Biomol. Struct.* **2004**, *33*, 720−731.
(3) Escribá, P. V. Membrane-Lipid Therapy: A New Approach in Molecular Medicine. *Trends Mol. Med.* **2006**, *12*, 34−43.
(4) In *Soft matter physics: an introduction*; Kleman, M., Lavrentovich, Ol. D., Eds.; Springer: New York, 2003.
(5) Osman, M. A.; Seyfang, G.; Suter, U. W. Two-Dimensional Melting of Alkane Monolayers Ionically Bonded to Mica. *J. Phys. Chem. B* **2000**, *104*, 4433−4439.
(6) Pimthon, J.; Willumeit, R.; Lendlein, A.; Hofmann, D. All-Atom Molecular Dynamics Simulation Studies of Fully Hydrated Gel Phase DPPG and DPPE Bilayers. *J. Mol. Struct.* **2009**, *921*, 38−50.
(7) Otero, R.; Gallego, J. M.; de Parga, A. L.V.; Martín, N.; Miranda, R. Molecular Self-Assembly at Solid Surfaces. *Adv. Mater.* **2011**, *23*, 5148−5176.
(8) Barth, J. V. Molecular Architectonic on Metal Surfaces. *Annu. Rev. Phys. Chem.* **2007**, *58*, 375−407.
(9) Barth, J. V.; Costantini, G.; Kern, K. Engineering Atomic and Molecular Nanostructures at Surfaces. *Nature* **2005**, *437*, 671−679.
(10) Berron, B.; Jennings, G. K. Loosely Packed Hydroxyl-Terminated SAMs on Gold. *Langmuir* **2006**, *22*, 7235−7240.
(11) Lahann, J.; Mitragotri, S.; Tran, T.-N.; Kaido, H.; Sundaram, J.; Choi, I.; Hoffer, S.; Somorjai, G. A.; Langer, R. A Reversibly Switching Surface. *Science* **2004**, *299*, 371−374.
(12) Park, J.-S.; Smith, A. C.; Lee, T. R. Loosely Packed Self-Assembled Monolayers on Gold Generated from 2-alkyl-2-methyl-propane-1,3-dithiols1,3-dithiols. *Langmuir* **2004**, *20*, 5829−5836.
(13) Thaxton, C. S.; Daniel, W. L.; Giljohann, D. A.; Thomas, A. D.; Mirkin, C. A. Templated Spherical High Density Lipoprotein Nanoparticles. *J. Am. Chem. Soc.* **2009**, *131*, 1384−1385.
(14) McMahon, K. M.; Mutharasan, R. K.; Tripathy, S.; Veliceasa, D.; Bobeica, M.; Shumaker, D. K.; Luthi, A. J.; Helfand, B. T.; Ardehali, H.; Mirkin, C. A.; Volpert, O.; Thaxton, C. S. Biomimetic High Density Lipoprotein Nanoparticles for Nucleic Acid Delivery. *Nano Lett.* **2011**, *11*, 1208−1214.
(15) Luthi, A. J.; Zhang, H.; Kim, D.; Giljohann, D. A.; Mirkin, C. A.; Thaxton, C. S. Tailoring of Biomimetic High-Density Lipoprotein Nanostructures Changes Cholesterol Binding and Efflux. *ACS Nano* **2012**, *6*, 276−285.
(16) Yang, S.; Damiano, M. G.; Zhang, H.; Tripathy, S.; Luthi, A. J.; Rink, J. S.; Ugolkov, A. V.; Singh, A. T. K.; Dave, S. S.; Gordon, L. I.; Thaxton, C. S. Biomimetic, Synthetic HDL Nanostructures for Lymphoma. *Proc. Natl. Acad. Sci. U.S.A.* **2013**, *110*, 2511−2516.
(17) Wang, Y.; Chen, G.; Yang, M.; Silber, G.; Xing, S.; Tan, L. H.; Wang, F.; Feng, Y.; Liu, X.; Li, S.; Chen, H. A Systems Approach towards the Stoichiometry-Controlled Hetero-Assembly of Nanoparticles. *Nat. Commun.* **2010**, *1*, 87.
(18) Cisneros, D. A.; Müller, D. J.; Daud, S. D.; Lakey, J. H. An Approach to Prepare Membrane Proteins for Single-Molecule Imaging. *Angew. Chem., Int. Ed.* **2006**, *45*, 3252−3256.
(19) Kim, P.; Lee, B. K.; Lee, H. Y.; Kawai, T.; Suh, K. Y. Molded Nanowell Electrodes for Site-selective Single Liposome Arrays. *Adv. Mater.* **2008**, *20*, 31−36.
(20) Nakamura, N.; Huang, H. X.; Qian, D. J.; Miyake, J. Quartz Crystal Microbalance and Electrochemical Studies on a Viologen Thiol Incorporated in Phospholipid Self-Assembled Monolayers. *Langmuir* **2002**, *18*, 5804−5809.
(21) Ulman, A. Formation and Structure of Self-Assembled Monolayers. *Chem. Rev.* **1996**, *96*, 1533−1554.
(22) Schreiber, F. Structure and Growth of Self-Assembling Monolayers. *Prog. Surf. Sci.* **2000**, *65*, 151−256.
(23) Love, J. C.; Estroff, L. A.; Kriebel, J. J.; Nuzzo, R. G.; Whitesides, G. M. Self-Assembled Monolayers of Thiolates on Metals as a Form of Nanotechnology. *Chem. Rev.* **2005**, *105*, 1103−1169.
(24) Vericat, C.; Vela, M. E.; Benitez, G.; Carrob, P.; Salvarezza, R. C. Self-Assembled Monolayers of Thiols and Dithiols on Gold: New Challenges for a Well-Known System. *Chem. Soc. Rev.* **2010**, *39*, 1805−1834.
(25) Smith, R. K.; Lewis, P. A.; Weiss, P. S. Patterning Self-Assembled Monolayers. *Prog. Sur. Sci.* **2004**, *75*, 1−68.
(26) Kenn, R.M.; Kjaer, K.; Möhwald, H. Non-Rotator Phases in Phospholipid Monolayers? *Colloid. Surf. A: Physicochem. Eng. Aspects* **1996**, *117*, 171−181.
(27) Matyszewska, D.; Sek, S.; Bilewicz, R. Electrochemical and Microscopic Characteristics of Thiolipid Layers as Simple Models of Cell Membranes. *Langmuir* **2012**, *28*, 5182−5189.
(28) Castner, D. G.; Hinds, K.; Grainger, D. W. X-ray Photoelectron Spectroscopy Sulfur 2p Study of Organic Thiol and Disulfide Binding Interactions with Gold Surfaces. *Langmuir* **1996**, *12*, 5083−5086.
(29) Heister, K.; Zharnikov, M.; Grunze, M.; Johansson, L. S. O. Adsorption of Alkanethiols and Biphenylthiols on Au and Ag

DOI: 10.1021/la504822q
Langmuir 2015, 31, 3232−3241

Substrates: A High-Resolution X-ray Photoelectron Spectroscopy Study. *J. Phys. Chem. B* **2001**, *105*, 4058−4061.
(30) Duwez, A.-S. Exploiting Electron Spectroscopies to Probe the Structure and Organization of Self-Assembled Monolayers: A Review. *J. Electron Spectrosc. Relat. Phenom.* **2004**, *134*, 97−138.
(31) Díaz-López, R.; Tsapis, N.; Libong, D.; Chaminade, P.; Connan, C.; Chehimi, M. M.; Berti, R.; Taulier, N.; Urbach, W.; Nicolas, V.; Fattal, E. Phospholipid Decoration of Microcapsules Containing Perfluorooctyl Bromide Used as Ultrasound Contrast Agents. *Biomaterials* **2009**, *30*, 1462−1472.
(32) Maroncelli, M.; Qi, S. P.; Strauss, H. L.; Snyder, R. G. Nonplanar Conformers and the Phase Behavior of Solid N-Alkanes. *J. Am. Chem. Soc.* **1982**, *104*, 6237−6247.
(33) Yee, C. K.; Ulman, A.; Ruiz, J. D.; Parikh, A.; White, H.; Rafailovich, M. Alkyl Selenide- and Alkyl Thiolate-Functionalized Gold Nanoparticles: Chain Packing and Bond Nature. *Langmuir* **2003**, *19*, 9450−9458.
(34) Le Bihan, T.; Pézolet, M. Study of the Structure and Phase Behavior of Dipalmitoylphosphatidylcholine by Infrared Spectroscopy: Characterization of the Pretransition and Subtransition. *Chem. Phys. Lipids* **1998**, *94*, 13−33.
(35) Atre, S. V.; Liedberg, B.; Allara, D. L. Chain Length Dependence of the Structure and Wetting Properties in Binary Composition Monolayers of OH- and CH_3-Terminated Alkanethiolates on Gold. *Langmuir* **1995**, *11*, 3882−3893.
(36) Valiokas, R.; Östblom, M.; Björefors, F.; Liedberg, B.; Shi, J.; Konradsson, P. Structural and Kinetic Properties of Laterally Stabilized, Oligo(Ethylene Glycol)-Containing Alkylthiolates on Gold: A Modular Approach. *Biointerphases* **2006**, *1*, 22−34.
(37) Bain, C. D.; E. Troughton, B.; Tao, Y.-T.; Evall, J.; Whitesides, G. M.; Nuzzo, R. G. Formation of Monolayer Films by the Spontaneous Assembly of Organic Thiols from Solution onto Gold. *J. Am. Chem. Soc.* **1989**, *111*, 321−325.
(38) Bain, C. D.; Whitesides, G. M. Formation of Monolayers by the Coadsorption of Thiols on Gold: Variation in the Length of the Alkyl Chain. *J. Am. Chem. Soc.* **1989**, *111*, 7164−7175.
(39) Fukuma, T.; Ichii, T.; Kobayashi, K.; Yamada, H.; Matsushige, K. True-Molecular Resolution Imaging by Frequency Modulation Atomic Force Microscopy in Various Environments. *Appl. Phys. Lett.* **2005**, *86*, 034103.
(40) Fukuma, T.; Kobayashi, K.; Horiuchi, T.; Yamada, H.; Matsushige, K. Alkanethiol Self-Assembled Monolayers on Au(111) Surfaces Investigated by Non-Contact AFM. *Appl. Phys. A: Mater. Sci. Process.* **2001**, *72*, S109−S112.
(41) Kaganer, V. M.; Möhwald, H.; Dutta, P. Structure and Phase Transitions in Langmuir Monolayers. *Rev. Mod. Phys.* **1999**, *71*, 779−819.
(42) Daillant, J.; Alba, M. High-Resolution X-Ray Scattering Measurements: I. Surfaces. *Rep. Prog. Phys.* **2000**, *63*, 1725−1777.
(43) Fenter, P.; Eisenberger, P.; Liang, K. S. The Chain Length Dependence of the Structure and Phases of $CH_3(CH_2)_{n-1}SH$ Self-Assembled on Au(111). *Phys. Rev. Lett.* **1993**, *70*, 2447−2450.
(44) Sirota, E. B.; King, H. E., Jr.; Singer, D. M.; Shao, H. H. Rotator Phases of the Normal Alkanes: An X-Ray Scattering Study. *J. Chem. Phys.* **1993**, *98*, 5809−5824.
(45) Sirota, E. B. Remarks Concerning the Relation between Rotator Phases of Bulk N-alkanes and Those of Langmuir Monolayers of Alkyl-Chain Surfactants on Water. *Langmuir* **1997**, *13*, 3849−3859.
(46) Hauser, H.; Pascher, I.; Pearson, R. H.; Sundell, S. Preferred Conformation and Molecular Packing of Phosphatidylethanolamine and Phosphatidylcholine. *Biochim. Biophys. Acta* **1981**, *650*, 21−51.
(47) Pascher, I.; Lundmark, M.; Nyholm, P.-G.; Sufide, S. Crystal Structures of Membrane Lipids. *Biochim. Biophys. Acta* **1992**, *1113*, 339−373.
(48) Nagle, J. F. Theory of the Main Lipid Bilayer Phase Transition. *Annu. Rev. Phys. Chem.* **1980**, *31*, 157−195.
(49) Singh, C.; Ghorai, P. K.; Horsch, M. A.; Jackson, A. M.; Larson, R. G.; Stellacci, F.; Glotzer, S. C. Entropy-Mediated Patterning of Surfactant-Coated Nanoparticles and Surfaces. *Phys. Rev. Lett.* **2007**, *99*, 226106.
(50) Singh, C.; Hu, Y.; Khanal, B. P.; Zubarev, E. R.; Stellacci, F.; Glotzer, S. C. Striped Nanowires and Nanorods from Mixed SAMS. *Nanoscale* **2011**, *3*, 3244−3250.
(51) Folkers, J. P.; Laibinis, P. E.; Whitesides, G. M.; Deutch, J. Phase Behavior of Two-Component Self-Assembled Monolayers of Alkanethiolates on Gold. *J. Phys. Chem.* **1994**, *98*, 563−571.
(52) Oyerokun, F. T.; Richard, A. V.; Maguire, J. F.; Barry, L. F. Role of Solvent Selectivity in the Equilibrium Surface Composition of Monolayers Formed from a Solution Containing Mixtures of Organic Thiols. *Langmuir* **2010**, *26*, 11991−11997.
(53) Stranick, S. J.; Parikh, A. N.; Tao, Y.-T.; Allara, D. A.; Weiss, P. S. Phase Separation of Mixed-Composition Self-Assembled Monolayers into Nanometer Scale Molecular Domains. *J. Phys. Chem.* **1994**, *98*, 7636−7646.
(54) Noh, J.; Kato, H. S.; Kawai, M.; Hara, M. Surface and Adsorption Structures of Dialkyl Sulfide Self-Assembled Monolayers on Au(111). *J. Phys. Chem. B* **2002**, *106*, 13268−13278.
(55) Gupta, B.; Ilg, P. Energetic and Entropic Contributions to the Landau−de Gennes Potential for Gay−Berne Models of Liquid Crystals. *Polymers* **2013**, *5*, 328−343.

DOI: 10.1021/la504822q
Langmuir 2015, 31, 3232−3241